Journal of Molecular Structure 1143 (2017) 91–99

Contents lists available at ScienceDirect

Journal of Molecular Structure

journal homepage: http://www.elsevier.com/locate/molstruc

Comparative study between 1-Propyl-3-methylimidazolium bromide and trimethylene bis-methylimidazolium bromide ionic liquids by FTIR/ATR and FT-RAMAN spectroscopies

Mohamed Kadari [a], El Habib Belarbi [a], Taqiyeddine Moumene [a, *], Serge Bresson [c], Boumediene Haddad [a], Ouissam Abbas [b], Brahim Khelifa [c]

[a] Laboratoire de Synthèse et Catalyse Tiaret LSCT, Univ Tiaret, BP 78 RP, 14000, Tiaret, Algeria
[b] Centre Wallon de Recherche Agronomique, CRA-W, Bâtiment Maurice Henseval, chaussée de Namur, 24, 50030, Gembloux, Belgium
[c] Laboratoire de Physique des Systèmes Complexes, Université Picardie Jules Verne, 33 rue S[t] Leu, 80039, Amiens cedex, France

ARTICLE INFO

Article history:
Received 14 November 2016
Received in revised form
15 April 2017
Accepted 17 April 2017
Available online 21 April 2017

Keywords:
Monocationic and dicationic ionic liquids
Imidazolium
Raman spectroscopy
FTIR/ATR spectroscopy

ABSTRACT

In this study, we synthesized two ionic liquids based on imidazolium: one is a monocationic and the other is a dicationic. They are respectively 1-Propyl-3-methylimidazolium bromide ([PrMIM$^+$][Br$^-$]) and trimethylene bis-methylimidazolium bromide ([M(CH$_2$)$_3$IM^{2+}][2Br$^-$]). The structures of these two ionic liquids which are composed of ions with atoms of the same nature were first identified by ^{1}H,^{13}C NMR, and then compared in a study by FT-RAMAN and FTIR/ATR spectroscopies.

FT-RAMAN spectras of the dicationic ionic liquid are richer in modes in the different spectral regions. Hence this richness seems to be a consequence of the passage from one to two rings in the imidazolium cation. In particular, the vibrational modes in the spectral ranges 700–600 cm^{-1}, 1700–1500 cm^{-1} and 3200–2700 cm^{-1} by FTIR/ATR seem to be sensitive to the change from mono to dicationic than in FT-RAMAN. The spectral range in which the intermolecular interactions are present (200-50 cm^{-1}) is a marker of differentiation between the mono and the dicationic. The spectral ranges on 1700–1200 cm^{-1} and 3200–2700 cm^{-1} also show signs of upheaval between our two samples. We can also notice that there are much more active modes in FT-RAMAN spectroscopy than in FTIR/ATR spectroscopy.

1. Introduction

Ionic liquids are liquids that consist almost exclusively of ions (an organic cation associated with an organic or inorganic anion). They are a class of salts with melting point temperature below a hundred degrees. J. M. Crosthwaite et al. noticed that the ionic liquids based on pyridinium become liquid around the 80 °C [1]. J. D. Holbrey and K. R. Seddon obtained the same results for ionic liquids based on imidazole [2]. In addition to their low melting points, ionic liquids are characterized by exceptional thermal stability, enabling their use for applications at high temperatures. They have a good ionic conductivity, generally of the order of 10^{-1}.S.m^{-1} [3]. Their electrochemical window is wide as they can provide tension between 5 and 6 V [4], which has been exploited in the field of fuel cells [5,6]. The Ionic liquids have also remarkable solvation capacities of organic and inorganic products comparable to polar solvents. Notwithstanding the fact that they are used as solvents in the biocatalytic reactions [7], it is most interesting to note that their physicochemical properties are adjustable by changing the nature of the anion and/or the cation (alkyl chain).

The applications of ionic liquids are dependent on their properties, while the latter dependent on the nature of the cation and anion combination and the length of the alkyl chains incorporated on the cation. The possible combinations of cations/anions are very numerous and continuously evolving, such that in general the properties of ionic liquids are governed by Coulomb forces, hydrogen bonding and Van der Waals interactions. In this paper, we will study two imidazolium-based ionic liquids.

In our study of both ionic liquids: a monocationic and dicationic which are respectively 1-Propyl-3-methylimidazolium bromide ([PrMIM$^+$][Br$^-$]) and trimethylene bis-methyl imidazolium bromide ([M(CH$_2$)$_3$IM^{2+}][2Br$^-$]), the nature of atoms constituting the anions and cations of both (ILs) are similar. However the difference is that the cation of the monocationic (IL) is constituted of a single

* Corresponding author.
E-mail address: taki407@yahoo.com (T. Moumene).

http://dx.doi.org/10.1016/j.molstruc.2017.04.076
0022-2860/

imidazolium ring while the cation of the dicationic consists of two imidazolium rings. So two singly charged cations linked by an alkyl chain and paired with two singly charged anions. In this study, we wanted to compare the vibrational behavior of these two ILs. Research conducted on the properties of ionic liquids and which is based on the understanding of the relationship between the structure of the cation and that of the anion aims at obtaining (ILs) with better properties whilst improving the theoretical model.

The study of the vibrational behavior of a material can be achieved by means of the following characterization techniques: FTIR spectroscopy, and RAMAN spectroscopy. These two non-destructive techniques are complementary and represent the best performing and most widely used tools. For monocationic ILs many studies have been carried out using these techniques [8,9]. This is not the case for dicationic ILs.

2. Experimental

2.1. Reagents and materials

The reagents used in this study are 1-methylimidazole (98 wt%), 1-bromopropane (99.5 wt%). They were purchased from Fluka and used as received.

2.2. NMR spectroscopy analysis

^{1}H NMR (400 MHz), ^{13}C NMR, spectra were recorded on a NMR 400 MHz spectrometer. The chemical shifts (δ) are given in ppm and referenced to the internal solvent signal, TMS (Tetramethylsilane) and $CFCl_3$, respectively.

2.3. Synthesis and characterization of ionic liquids

2.3.1. Synthesis of ([PrMIM$^+$][Br$^-$])

The synthesis was prepared according to procedures describe in the literature. Briefly, 1-methylimidazole (6.79 ml, 85.26 mmol), and 1-bromopropane (9.87 ml, 89.03 mmol) were combined at a 1:1 ratio before being stirred at 70 °C for 6 h. The [PrMIM$^+$][Br$^-$] was then washed with ethyl acetate to remove any excess reactants or contaminants. Subsequently, about 20 ml of ethyl acetate was added to the [PrMIM$^+$] [Br$^-$] and the mix shaken together in a separatory funnel. After a few minutes, the mixture separated into two distinct layers; the top layer being ethyl acetate and all of the contaminants and the bottom layer was [PrMIM$^+$] [Br$^-$]. The top layer, which was discarded later, was poured into a clean beaker. The bottom layer was saved in the original flask. This washing procedure was repeated four times.

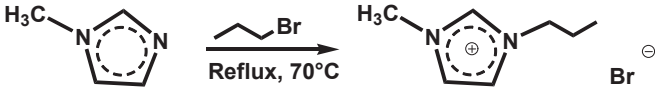

2.3.2. Synthesis of ([M(CH$_2$)$_3$IM^{2+}][2Br$^-$])

In a flask of 100 ml, we prepared a mixture of 1-methyl imidazole (9.07 ml, 100 mmol) and 1,3-dibromopropane (5.21 ml, 49.98 mmol) and 23 ml of DMF. This reaction mixture is heated under reflux with magnetic stirring for 4 h while maintaining the temperature at 75 °C. Bromide trimethylene bis-methyl imidazolium was obtained as a slightly yellow solid (6.60 g, 17.12 mmol) with a yield of 63%.

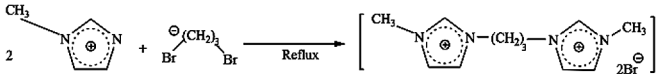

2.4. NMR results

The spectra details are given below,

^{1}H NMR ($CDCl_3$) δ_H (ppm) **[PrMIM$^+$][Br$^-$]**: 10.27 (1H, s, N$^+$C**H**N), 7.58 (1H, s, N$^+$CHC**H**NCH$_3$), 7.49 (1H, s, N$^+$C**H**CH), 4.26 (3H, s, N**CH$_3$**), 1.95–1.93 (2H, m, N$^+$C**H$_2$**CH$_2$), 1.87–1.85 (2H, m, CH$_2$C**H$_2$**CH$_3$), 0.91 (3H, t, J = 6.8 Hz, N$^+$(CH$_2$)$_2$C**H$_3$**).

^{13}C NMR ($CDCl_3$) δ_C (ppm) **[M(CH$_2$)$_3$IM^{2+}][2Br$^-$]**: 10.67 (CH$_2$CH$_2$**C**H$_3$), 32.62 (CH$_2$**C**H$_2$CH$_3$), 36.62 (N**C**H$_3$), 51.35 (N$^+$**C**H$_2$CH$_2$), 122.32 (N**C**HCHN$^+$), 123.75 (NCH**C**HN$^+$), 137.01 (N$^+$**C**HN).

2.5. FTIR/ATR and FT-RAMAN measurements

The measurements were realised in the Walloon Agricultural Research Center (CRA-W) Belgium.

2.5.1. FTIR/ATR measurements

All attenuated total reflectance Fourier transform mid-infrared (ATR/FTIR) spectra were obtained on a Vertex 70-RAM II Bruker spectrometer (Bruker Analytical, Madison, WI) operating with a Golden Gate TM diamond ATR accessory (Specac Ltd, Slough, UK).

FTIR/ATR spectra [4000-600 cm^{-1}] were collected with a resolution of 1 cm^{-1} by co-adding 64 scans for each spectrum. The OPUS 6.0 software for windows of Bruker Instruments was used for instrument management.

2.5.2. FT-RAMAN measurements

FT-RAMAN spectra were obtained on a Vertex 70-RAM II Bruker FT-RAMAN spectrometer. This instrument is equipped with a Nd: YAG laser (yttrium aluminium garnet crystal doped with triply ionized neodymium) with a wavelength for incident laser at 1064 nm (9398,5 cm^{-1}). The maximum laser power was 1.5 W. The measurement accessory was pre-aligned, only the Z-axis of the scattered light was adjusted to set the sample in the appropriate position relation to the local point. The RAM II spectrometer is equipped with a liquid-nitrogen cooled Ge detector. FT-RAMAN spectra [4000-45 cm^{-1}] were collected with a resolution of 1 cm^{-1} by co-adding 256 scans for each spectrum. The OPUS 6.0 software was used for the spectral acquisition, manipulation and transformation.

3. Results and discussion

3.1. Comparison between the FTIR/ATR spectra of ionic liquids: ([PrMIM$^+$][Br$^-$]) and ([M(CH$_2$)$_3$IM^{2+}][2Br$^-$])

Table 1 below shows the observed FTIR/ATR bands and their assignments in the spectral region of 600 cm^{-1} to 3420 cm^{-1} of two ionic liquids mono and di-cationic [PrMIM$^+$] [Br$^-$] and ([M(CH$_2$)$_3$IM^{2+}][2Br$^-$]). Figs. 1–3 show the infrared spectra of the two samples in the spectral regions 1200 cm^{-1} to 600 cm^{-1}, 1800 cm^{-1} to 1200 cm^{-1} and 3700 cm^{-1} to 2700 cm^{-1} respectively. There are 30 peaks in this zone for the dicationic and 34 peaks for the monocationic.

3.1.1. The region 1200-600 cm^{-1}

Almost the same number of peaks were observed for the two samples in this spectral zone: 15 peaks for the monocationic and 13 peaks for the dicationic. Although the spectra of these two samples are similar, there are peaks in the spectrum of the mono that do not exist in the spectrum of dicationic, and vice versa. With regard to the modes present in the two spectra, some peaks which have undergone wavenumber shifts of the order of 4 cm^{-1} were observed. The Peaks at 620, 694, 756, 1022 and 1165 cm^{-1} for the dicationic corresponded respectively to the peaks at 618, 696, 752,

Table 1
Observed FTIR/ATR bands of ([PrMIM$^+$][Br$^-$]) and ([M(CH$_2$)$_3$IM^{2+}][2Br$^-$]) and their assignments (vw = very weak; w = weak; m = medium, s = strong; sh = shoulder; ν = str = stretching; δ = def = deformation; bend = bending deformation; ω = wagging; ρ = rocking; γ = bending out-of-plane; t = twist = twisting, s = symmetric; as = antisymmetric, * = fitted value).

[M(CH$_2$)$_3$IM^{2+}][2Br$^-$]	[PrMIM$^+$][Br$^-$]	Vibrational assignment	Refs.
620 (vs)	618 (s)	CH$_3$(N)CN str	[12]
639 (m)		γ(N–H)	[17]
647 (m)	649 (m)	CH$_3$NCN str	[9]
660 (m)	660 sh	CH def–vib, NH$_2$ wagging vib	[15]
694 (w)	696 (w)	Out-of-plane C–H def vib	[15]
714 (w)		CH$_2$(N) and CH$_3$(N)CN str	[10]
756 (m)	752 (m)	δHCCH/Ring HCCH *asym* bend/ω(C–H)	[8]/[13]
	800 (m)	Ring HCCH *asym* bend/CH$_2$ rocking def- vib	[8]/[15]
826 + 836 (m)	827 (m)	NC(H)N bend/CCH bend/ω(CH$_2$) and ω(CH)	[12]/[11]
	864 (m)	ω(C–H)/CH$_2$ out-of-plane def vib	[11]/[15]
	900 (w)	C–H out-of-plane vib/CH$_2$ rocking vib	[15]
	1010 (w)	ν(C–C)/ρ(C–H) [ip]/CH$_3$ rocking vib	[11]/[15]
1022 (w)	1019 (w)	ρ(CH$_2$), t(CH$_2$)/CH$_3$ rocking vib and CN str	[11]/[15]
1062 (w)	1049 (w)	CC str, NCH$_3$ twist/CH$_3$ rocking vib	[8]/[15]
1097 (m)	1089 (w)	CC str/ρ(N–C)	[12]/[11]
	1116 (w)	ρ(C–H)	[11]
1165 (vs)	1168 (vs)	CH$_2$(N) and CH$_3$(N)CN str, CC str	[8]
	1230 (vw)	CH$_2$ twisting vib/ν(CC)	[15]/[17]
1253 (vw)		t(CH$_2$)/CH$_2$ wagging vib.	[17]/[15]
	1272 (w)	CH$_2$ wagging vib/ρ(C–H)	[15]/[11]
	1297 (w)	CH$_2$ twisting vib/γ(C–H)	[17]
1339 (w)	1336 (w)	CH$_2$(N) and CH$_3$(N) CN str	[8]
	1345 (w)	CH$_2$(N), CH$_3$(N) CN str	[8]
1389 (m)	1385 (w)	CH$_2$(N) CN bend, CH$_2$(N) and CH$_3$(N) CN str/ρ(N–H)	[8]/[13]
	1428 (w)	CH$_3$ (N) str, CH$_3$ (N) HCH *sym* bend or NC(CH$_3$)N HCH bend	[8]
1458 (m)	1458 (m)	δ(CH$_2$)/CCH HCH *asym* bend, CH$_3$(N)HCH *sym* bend, CH$_3$(N) str	[18]/[12]
1562 (s)	1564 (s)	ν(N=C)/ρ(C–H)	[11]
1574 (s)	1570 (s)	ring ip *sym*/asym str, CH$_3$(N) str, CH$_2$(N) CN str	[12]
1655 (s)		ν(C=C), ν(C–N), δ(N–H)	[17]
2858 (vw)	2859*	ν$_s$(CH$_2$)	[17]
	2876 (w)	ν$_{as}$(CH$_2$)	[18]
2928* sh	2933* sh (m)	ν$_s$(CH$_3$)	[18]
2952 (w)	2964 (m)	ν$_{as}$(CH$_2$HCH)	[8]/[12]
3030* sh	3014* sh	ν(C–H)	[11]
3085 (m)	3062 (m)	ν(C–H)	[11]
3145 (m)	3140 (w)	ν(C–H)	[8]
3245* sh		Free N–H str	[15]
3362* sh	3385* (w)	Free N–H str	[15]
3430 (s)	3450* (w)	Free N–H str	[15]
3495* sh		Free N–H str	[15]

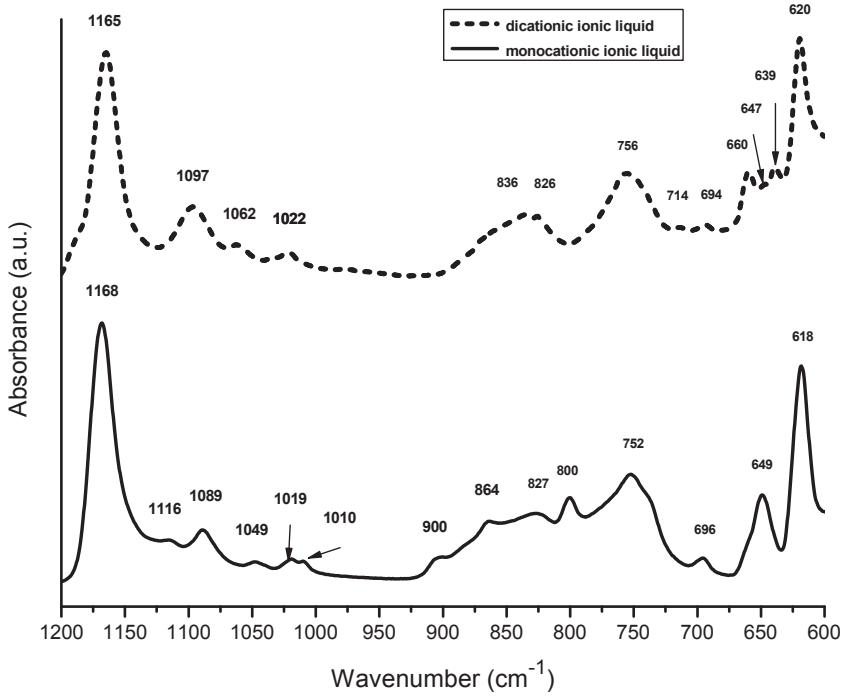

Fig. 1. FTIR/ATR spectra of: [PrMIM$^+$][Br$^-$] and ([M(CH$_2$)$_3$IM^{2+}][2Br$^-$]) in the region 1200–600 cm^{-1}.

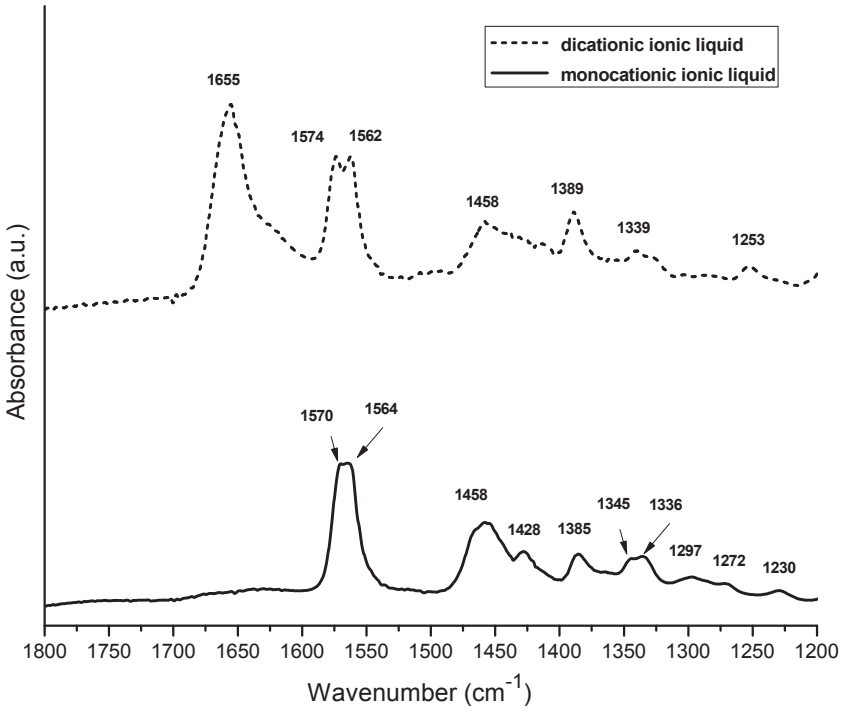

Fig. 2. FTIR/ATR spectra of: ([PrMIM$^+$][Br$^-$]) and ([M(CH$_2$)$_3$IM^{2+}][2Br$^-$]) in the region from 1800 to 1200 cm^{-1}.

1019 and 1168 cm^{-1} for the monocationic. These peaks are assigned to the stretching vibration of CH$_3$(N)CN and CH$_2$(N) bonds [8,9,12] and C–N stretching [15]. It is also noted that in the region 675-635 cm^{-1} the peak at 649 cm^{-1} with a shoulder at 660 cm^{-1} became a triplet for the case of dicationic ionic liquid: 639, 647 and 660 cm^{-1}. Therefore the passage from one to two rings imidazolium has an influence on the vibrational behavior of ring bonds. Furthermore the following observations were made: deformation (HCCH) and wagging (C–H) for 752 cm^{-1} [13], stretching (C–C) for 1168 cm^{-1} [11], rocking (CH$_2$ and CH$_3$) and twisting (CH$_2$) for 1019 cm^{-1} [11] and out-of-plane C–H def-vib for 696 cm^{-1} [15]. Therefore, this passage also has an effect on the vibrational modes of other bonds of the cation. Other peaks underwent more important wavenumber shifts of the order of 12 cm^{-1}, for example the peaks at 1062 and 1097 cm^{-1} for the dicationic corresponded to the ones at 1049 and 1089 cm^{-1} for the monocationic. In the literature, these peaks are attributed to the stretching vibration of the (C–C) bond [8,12], the rocking of the (N–C) [11] and the twisting of NCH$_3$ [8] indicating that this zone is very sensitive to the passage of the mono to dicationic ionic liquid.

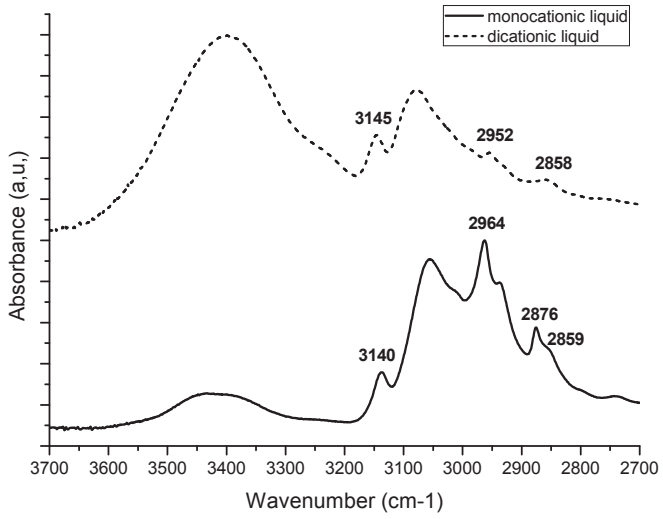

Fig. 3. FTIR/ATR spectra of: ([PrMIM$^+$][Br$^-$]) and ([M(CH$_2$)$_3$IM^{2+}][2Br$^-$]) in the region 3700–2700 cm^{-1}.

3.1.2. The region 1800-1200 cm^{-1}

In this spectral region, there were more peaks in the case of monocationic than in the case of dicationic, which can be explained by a congestion masking certain vibrational modes for the dicationic. The monocationic spectrum peaks are a little broader than the dicationic ones, suggesting more order in the dicationic structure. We observed a very intense new peak at 1655 cm^{-1} in the case of dicationic. In the literature, this peak is attributed to stretching vibration of (C=C) and (C–N) bonds, and deformation of (N–H) bond [17]. Its appearance and its intensity can be explained by the increase in the number of these bonds ((C=C), (C–N), (N–H)) that represent a signature of the passage of the mono to dicationic ionic liquid.

3.1.3. The region 3700-2700 cm^{-1}

In this region, almost the same number of peaks for both samples was seen, 9 peaks for the monocationic and 10 peaks for the dicationic. The spectral band between 3500 and 3200 cm^{-1} was much higher in intensity for the dicationic compared to the monocationic. An actual rollover was observed in intensity in the spectral regions 3200-2800 cm^{-1} and 3500-3200 cm^{-1} between the monocationic and dicationic. This phenomenon was explained by computing different intensity ratios shown in Table 2 by referring to the peak at 2955 cm^{-1}. The increase in intensity is obvious, especially on the modes corresponding to ν(CH) at 3145 cm^{-1} [8] and ν(NH) at 3430 cm^{-1}. The number of vibrational modes in the spectral region 3500-3200 cm^{-1} also increased, 2 modes for monocationic, 4 modes for dicationic assigned to ν(NH). All these

Table 2
Reports of intensity of many peaks of **[PrMIM$^+$][Br$^-$]** and **[M(CH$_2$)$_3$IM^{2+}][2Br$^-$]** in the spectral range 3500–2800 cm^{-1}.

Mono or dicationic ionic liquid	I_{2850}/I_{2955}	I_{3075}/I_{2955}	I_{3145}/I_{2955}	I_{3430}/I_{2955}
[PrMIM$^+$][Br$^-$]	0.48 ± 0.02	0.92 ± 0.02	0.36 ± 0.02	0.20 ± 0.02
[M(CH$_2$)$_3$IM^{2+}][2Br$^-$]	0.68 ± 0.02	1.68 ± 0.02	1.16 ± 0.02	2.27 ± 0.02

variations seem to be explained by the increased number of N–H bonds (see Fig. 4).

3.2. Comparison between FT-RAMAN spectra of ionic liquids ([PrMIM$^+$][Br$^-$]) and ([M(CH$_2$)$_3$IM^{2+}][2Br$^-$])

Table 3 below represents the observed FT-RAMAN bands and their assignments for both ionic liquids ([PrMIM$^+$][Br$^-$]) and ([M(CH$_2$)$_3$IM^{2+}][2Br$^-$]). Figs. 5–8 show the FT-RAMAN spectra of the two samples in the spectral regions 1000 cm^{-1} to 45 cm^{-1}, 200 cm^{-1} to 45 cm^{-1}, 1700 cm^{-1} to 1000 cm^{-1} and 3200 cm^{-1} to 2700 cm^{-1} respectively. We noticed that the FT-RAMAN spectrum of dicationic was richer in vibrational modes than that of monocationic: 75 peaks for the dicationic and 38 picks for the monocationic.

3.2.1. The region 200-45 cm^{-1}

In this region an important difference between the two spectra was observed. The spectrum of the monocationic ionic liquid had a wideband with a single peak that characterizes the amorphous phase, while the spectrum of dicationic ionic liquid showed several peaks, indicating in this case the presence of a crystalline phase.

The slight swinging motion of the imidazolium ring, an absent phenomenon in the non-aromatic ionic liquids must be expressed in the RAMAN spectra of both ionic liquids: a broad peak at ≈57 cm^{-1} in the case of monocationic ionic liquid, which becomes relatively narrow at 86 cm^{-1} in the case of dicationic, due here to the presence of the crystalline phase. Furthermore the results of C. Penna et al. [14] indicate that the RAMAN spectrum must present other peaks attributed to the mode linked to the rocking motion: 146 cm^{-1} and 189 cm^{-1} (the wavenumber 189 cm^{-1} from the literature can also be attributed to twisting of the bond (N–C) or to rocking (CH$_2$) [11]). The number and intensities of the peaks show the influence of the passage of a monocationic ionic liquid to a dicationic ionic liquid. The peaks at 100 cm^{-1} and 127 cm^{-1} are attributed to intramolecular interactions [14].

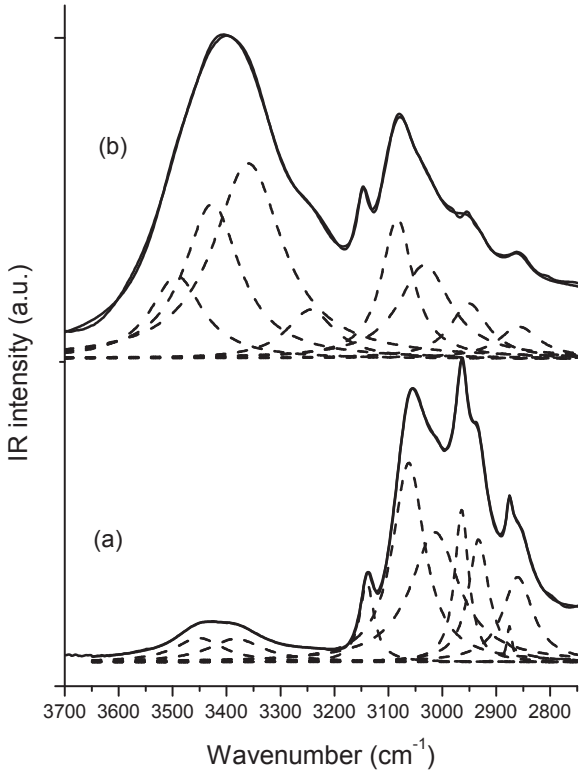

Fig. 4. The Results of Lorentzian curve fitting of FTIR/ATR spectra for: (a) ([PrMIM$^+$][Br$^-$]) and (b) ([M(CH$_2$)$_3$IM^{2+}][2Br$^-$]) in the region 3700–2700 cm^{-1}.

The frequencies ≈57 cm^{-1}, ≈68 cm^{-1} and ≈80 cm^{-1} are attributed to partial character of acoustic excitations for a crystalline physical state (intermolecular vibrational modes) [14]. This character is compatible with the fact that we found these vibrational modes regardless of the specific molecular structure. Therefore, these modes are also independent of the alkyl chain length of the cation, either be it an aromatic or a non-aromatic ionic liquid. On the other hand, these modes depend on the strength of the cation-anion interactions. Penna et al. [14] studied two monocationic ionic liquids [C$_6$C$_1$im][Tf$_2$N] and [C$_6$C$_1$im]Br in crystalline phase. When passing from [C$_6$C$_1$im][Tf$_2$N] to [C$_6$C$_1$im]Br, they noticed in this zone of low frequencies a wavenumber shift of about 10 cm^{-1}, which shows the influence of the nature of the anion. Moreover, for our dicationic ionic liquid which represents the crystalline phase and at the same time their cations, they contain two imidazolium rings. We also registered a wavenumber shift with a higher order than the previous, which indicates that the number of cycles in the imidazolium cation also has an influence on the modes of intermolecular vibrations.

3.2.2. The region 1000-200 cm^{-1}

In this region, there were 14 peaks for the monocationic ionic liquid and 23 peaks for the dicationic, indicating, for the latter, a richer RAMAN spectrum in vibration modes.

While passing from the monocationic ionic liquid to the dicationic ionic liquid, we observed the appearance of several new peeks: at 256 and 267 cm^{-1}, attributed to rocking mode of the (N–C) bond [11], and at 299 cm^{-1} attributed to modes CH$_2$(N) and CH$_3$(N)CH bend [8]. In addition several other more or less intense peaks: 429, 641, 718, 781, 829, 841, 892 and 976 cm^{-1}were observed. At 613 cm^{-1} a peak was present with medium intensity assigned to ω(NH) mode, the stretching of (CH$_2$) or (CH$_3$(N)CN) [12].

We also noticed deconvolutions of peaks: 621 cm^{-1} in the case of the monocationic which corresponded to a doublet 621 and 624 cm^{-1} in the case of dicationic,is attributed to the vibration mode in the plane (stretching of the (N–CH$_3$) bond) [11]. The peak at 868 cm^{-1} in the case of monocationic became a doublet for the dicationic: 872 and 884 cm^{-1} with a shoulder at 865 cm^{-1}, all assigned to vibrations NC(H)N bend and CCH bend [13].

We observed for the other peaks minor wavenumber shifts of the order of 2 cm^{-1} (from 316 cm^{-1} for the mono to 317 cm^{-1} for the dicationic, from 661 cm^{-1} to 663 cm^{-1} and 697 to 695 cm^{-1}), the peak at 418 cm^{-1} remained unchanged for mono and dicationic. Still there were two peaks with remarkable wavenumber shifts (from 461 cm^{-1} to 475 cm^{-1} assigned to (C–H) stretching [15] and

Table 3
Observed FT-RAMAN bands and their assignments (vw = very weak; w = weak; m = medium, s = strong; sh = shoulder; ν = str = stretching; δ = def = deformation; bend = bending deformation; ω = wagging, ρ = rocking, τ = torsion; t = twist = twisting; β = bending in-plane, s = symmetric; as = antisymmetric, [ip] = in plane, [op] = out of plane).

$[M(CH_2)_3IM^{2+}][2Br^-]$	$[PrMIM^+][Br^-]$	Vibrational assignment	Refs.
57 (s)	57 (vs)	Intermolecular vibration	[14]
68 (s)		Intermolecular vibration	[14]
80 (s)		Intermolecular vibration	[14]
86 (vs)		Intermolecular vibration	[14]
100 (s)		Intramolecular vibration	[14]
127 (m)		Intramolecular vibration	[14]
146 (m)		Intermolecular vibration	[14]
189 (m)		Intermolecular vibration/τ(N–C)/ρ(CH_2) 1 as ðR6þ,	[14]/[11]
	228 (vw)	β(CCC)	[11]
256 sh + 267 (w)		ρ(N–C)	[11]
	282 (vw)	CH_3 torsional vib	[15]
299 (vw)		CH_2(N) and CH_3(N)CH bend	[8]
317 (vw)	316 (vw)	CH_2(N) and CH_3(N)CH bend	[8]
	365 (vw)	ν(C–C)	[11]
418 (m)	418 (vw)	t(CH_2)	[11]
429 (vw)		CC def vib [op]	[15]
475 (w)	461 (vw)	ν(C–H)	[15]
595 (vw)	601 (w)	ω(N–C)	[11]
613 (m)		ω(N–H)/CH_2 str, CH_3(N)CN str	[10]/[12]
621sh + 624 (w)	621 (w)	ν (N–CH_3) [ip]	[11]
641 (vw)		ρ(CH_2), ρ(CH)	[11]
663 (m)	661 (vw)	ρ(CH_2)	[11]
695 (w)	697 (vw)	ω(C–H)	[11]
718 (vw)		CH_2 rocking	[15]
	738 (vw)	CH def-vib	[15]
781 (w)		ν_s(CC), ring HCCH *sym* bend, NC(H)N *sym* [op] bend	[8]
	803 (vw)	Ring HCCH *sym* bend, NC(H)N bending [op]	[8]
829 + 841 (w)		CH def vib [op]	[15]
865 sh + 872+884 (w,m)	868 (w)	NC(H)N bend/CCH bend	[13]
892 (vw)		CH def vib [op]/CH_3 rocking vib	[15]
	905 (vw)	CH def vib [op]	[15]
976 (w)		ν(CC), ring *asym* bend [ip]	[12]
1010 + 1018 (s)	1012 sh + 1021 (m)	ν(C–C)/ρ(C–H)	[11]
1029 (m)		CH_3(N) str, CH_2(N) str/ρ(C–H)	[12]/[11]
1039 (m)	1045 (w)	CH_3(N) str, CH_2(N) str/ν(N–C)	[12]/[11]
1056 (vw)		ν(N–C)/ν(CC), ring CN *asym* ip str [ip]	[11]/[8]
1094 (w)	1094 sh (w)	ν(CC), ring HCCH *sym* bend, ring *sym* bend [ip]	[12]
1107 (m)	1116 (w)	ν(CC), ring HCCH *sym* bend, ring *sym* str [ip]	[12]
1123 (w)		ν(CC)	[13]
1163 (vw)	1173 (vw)	ρ(CH)	[11]
1189 (vw)		ρ(CH)	[11]
1207 (vw)		γ(CH) [op],ρ(CH_2),ν(CC) [ip]	[17]
	1228 (vw)	ν(C–N), ρ(N–H)	[11]
1277 (m)	1272 (vw)	ρ(C–H) [ip], t(CH_2) [ip]	[17]
1291 (vw)	1295 (vw)	t(CH_2) [op],γ(CH)	[17]
1307 (w)		t(CH_2) [op], γ(CH) ring	[17]
1333 (m)	1336 (m)	Ring *sym* str [ip], CC str, CH_2(N) and CH_3(N) CN str CH 3 (N) CN str	[8]
1346 (m)		Ring *sym* str [ip], CC str, CH_2(N) and CH_3(N) CN str CH 3 (N) CN str	[8]
1358 (w)		ρ(CH_2), ρ(CH)/CH_2(N) str, ν(CC), CH_2(N)CN str	[11]/[12]
1365 (w)		ρ(CH_2), ρ(CH)	[11]
1382 + 1386 (m)	1385 (m)	ρ(CH_2), ρ(CH)/δ(CH_2) [op], ω(CH), ω(NH)	[11]/[17]
1410 sh + 1415+1428 (m,s,vs)	1416 (s)	CH_2(N)/CH_3(N)CN str	[13]
1439 (m)		δ(CH_2)	[13]
1443 sh (m)		CH_3(N) HCH *sym* bend/δ(CH)	[8]/[11]
1460 (m)	1454 (m)	CCH HCC *sym* bend, CH_3(N)HCH *sym* bend	[12]
1467 (m)	1469 (m)	ν(N–C), δ(CH_2)	[11]
1557 sh + 1565+1575 sh (vw,w,vw)	1564 (w)	ν(N–C)/CH_2(N) and CH_3(N) CN str	[11]/[8]
2708 (vw)		CH def-vib [ip]	[15]
2755 (vw)	2748 (vw)	ν_s(CH_3)	[15]
2811 (vw)		ν_s(CH_3)/ν_{as}(CH_3)	[15]
2837 (vw)	2828 (w)	ν_s(CH_2)/ν_s(CH_3)	[13]/[15]
	2876 (s)	ν_s(CH_2)/CH_3HCH *sym* str/ν_{as}(CH_2)	[17]/[12]/[13]
2896 (m)	2898 (m)	ν_s(CH_3)/ν_{as}(CH_2), ν_s(CH_2)	[15]/[17]
2928 (m)		Ring CH_3HCH *sym* str	[12]
2948 (s)	2943 (vs)	ν_{as}(CH_2), ν(CH)	[17]

Table 3 (*continued*)

$[M(CH_2)_3IM^{2+}][2Br^-]$	$[PrMIM^+][Br^-]$	Vibrational assignment	Refs.
	2972 sh (s)	CH_2HCH *asym* str, ethyl HCH *asym* str	[12]
2982 + 3000 sh (m)		$\nu_{as}(CH_3)$/N–H str	[13]/[15]
3045 (w)		ν(C–H)	[13]
	3063 (w)	ν(C–H)	[13]
3087 + 3098 (w)		ν(C–H)/CH_3(N)HCH *asym* Str	[11]/[13]
3136 (vw)	3138 (vw)	ring (HCCH and N–(C–H)–N) C–H str/ν(C–H)	[16]/[13]
3156 (vw)		ring (HCCH and N–(C–H)–N) C–H str/ν(C–H)/ν(N–H)	[16]/[13]/[15]

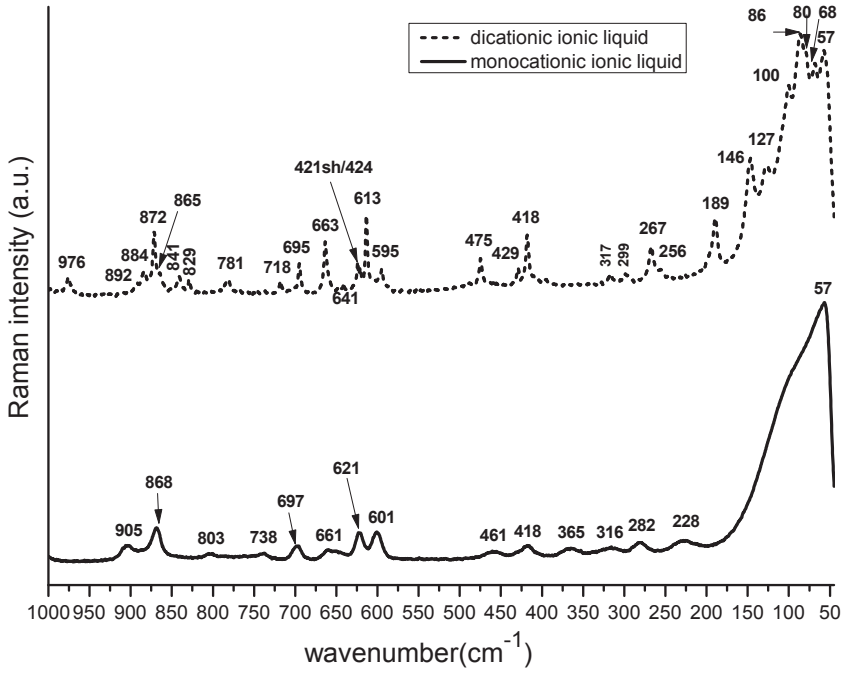

Fig. 5. The FT-RAMAN spectra of: $[PrMIM^+][Br^-]$ and $([M(CH_2)_3IM^{2+}][2Br^-])$ in the region 1000–1045 cm^{-1}.

from 601 cm^{-1} to 595 cm^{-1} assigned to ω(N–C) [11]).

3.2.3. The region 1700-1000 cm^{-1}

In this region, we observed 30 peaks for the dicationic versus 15 peaks for the monocationic. So also in this region, the spectrum of dicationic is richer in modes than the spectrum of monocationic. New peaks appeared in the case of dicationic: two less intense peaks at 1056 cm^{-1} and 1358 cm^{-1}, other peaks slightly more intense at 1029, 1123, 1189, 1207, 1307, 1346, 1365, 1439 cm^{-1} and a shoulder at 1443 cm^{-1}, the assignments of these peaks are in Table 3. Among these peaks the most remarkable one is at 1346 cm^{-1} assigned to Ring *sym* str [ip], CC str, CH_2(N) and CH_3(N) CN str [8].

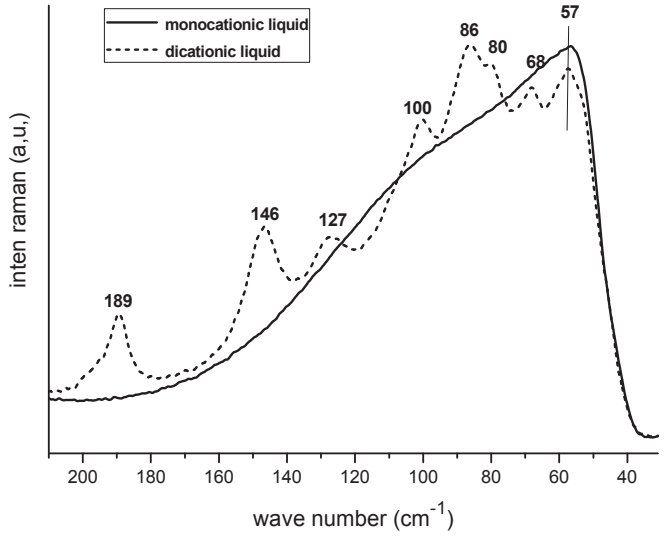

Fig. 6. The FT-RAMAN spectra of $[PrMIM^+]$ $[Br^-]$ and $([M(CH_2)_3IM^{2+}][2Br^-])$ in the region 200–45 cm^{-1}.

Deconvolutions of the peaks was also observed in this region. The peak at 1385 cm^{-1} for mono became a doublet for the dicationic: 1382 and 1386 cm^{-1}. These peaks are attributed in the literature to the CH bond vibration or the NH bond [8,17]. The peak at 1416 cm^{-1} changed into a triplet: 1410 cm^{-1}, 1415 cm^{-1} and 1428 cm^{-1}. These peaks are assigned to the stretching vibration of CH_2(N) and CH_3(N) CN [13]. Also a peak at 1564 cm^{-1} changed into a triplet: 1557 cm^{-1}, 1565 cm^{-1} and 1575 cm^{-1}. These frequencies are also attributed to stretching vibration of CH_2(N) and CH_3(N) CN [8] and ν(N–C) [11]. For the rest of the peaks, we observed more or less significant shifts of the order of 2 cm^{-1} to 10 cm^{-1}.

It is also envisaged that the peaks of the RAMAN spectrum of the dicationic are narrower than for the monocationic, which means that it has more order in the dicationic structure than the monocationic.

3.2.4. The region 3200-2700 cm^{-1}

As in previous regions, in region 3200-2700 cm^{-1}, the dicationic

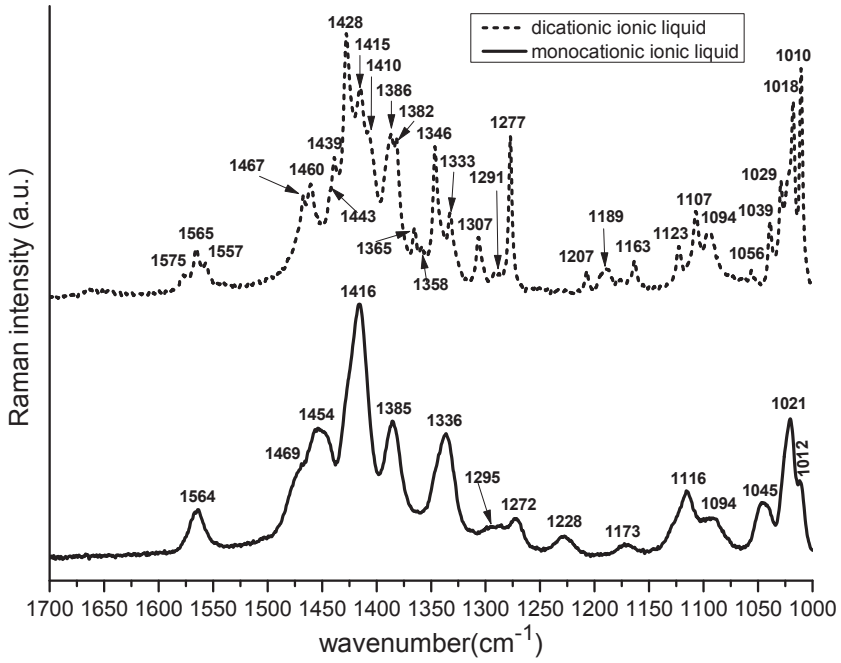

Fig. 7. FT-RAMAN spectra of: [PrMIM$^+$][Br$^-$] and ([M(CH$_2$)$_3$IM^{2+}][2Br$^-$]) in the region 1700–1000 cm^{-1}.

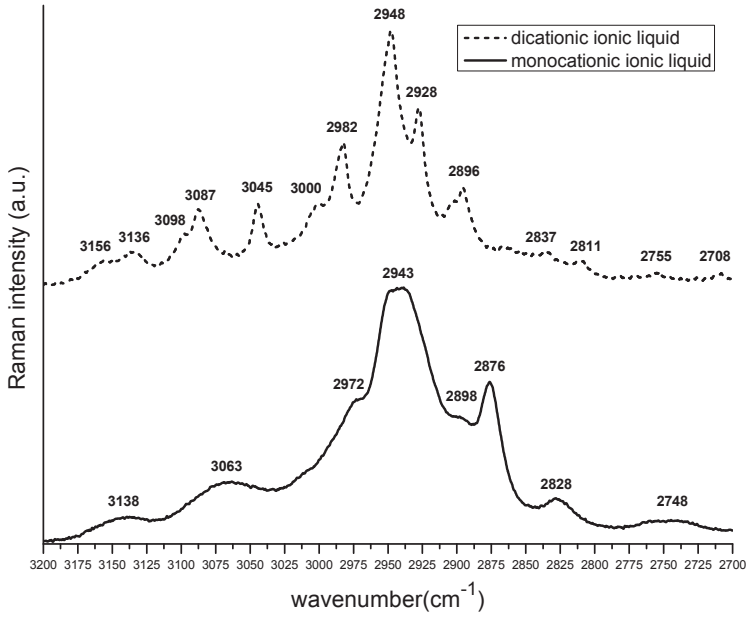

Fig. 8. The FT-RAMAN spectra of: [PrMIM$^+$] [Br$^-$] (monocationic) and ([M(CH$_2$)$_3$IM^{2+}][2Br$^-$]) (dicationic), in the region 3200–2700 cm^{-1}.

spectrum was richer in vibration modes than the monocationic one, with 14 peaks versus 8 peaks observed. New peaks were present at 2708 cm^{-1} (assigned to CH in-plane def-vib), 2811 cm^{-1} (assigned to *sym* CH_3 str, *asym* CH_3 str), 2928 cm^{-1} (assigned to ring CH_3HCH *sym* str), 2982 cm^{-1} and 3000 cm^{-1} (assigned to $\nu_{as}(CH_3)$), 3045 cm^{-1}, 3087 cm^{-1} and 3098 cm^{-1} (assigned to ν(CH)), and 3156 cm^{-1} (assigned to the ring (HCCH and N(CH)N)CH str/ν(CH)). In the literature 2982 cm^{-1}, 3000 cm^{-1} and 3156 cm^{-1} are attributed to the stretching vibration of NH bond. For modes present in both spectra, we had a frequency shift of the order of 2 cm^{-1} to 9 cm^{-1}.

Therefore, all spectral regions of the FT-RAMAN spectrum that we saw above show sensitivity towards the passage of mono to dicationic by more peaks in the case of dicationic and wavenumber shifts.

4. Conclusion

This study showed that in passing of an imidazolium-based monocationic (IL) where the cation is composed of a one imidazolium ring to a dicationic (IL) where the cation is composed of a two imidazolium rings, there is a change of environment for ions, hence more or less freedom of movement. This was expressed on the FT-RAMAN spectrum in a wide spectral region by the

appearance of new vibrational modes (37 new peaks), deconvolutions and wavenumber shifts, which can serve as a signing of differentiation between these (ILs).

This change in the number of imidazolium rings in the cation also influences the intermolecular (anion-cation interaction) and intramolecular vibration modes. Indeed in the spectral zone 200-45 cm^{-1}, representative of these modes, we could see: a broadband with only a single peak for the monocationic, characteristic of an amorphous phase, versus several peaks for the dicationic, characteristic of a crystalline phase. So the self-organization known to ionic liquids was manifested in the case of dicationic. Therefore, this spectral zone is a signature of the physical state of the (IL), than the change of the number of imidazolium rings in the cation.

We note that for the FTIR/ATR spectroscopy the clutter of ions masked certain vibration modes for the dicationic. Yet, we had more or less important wavenumber shifts, peaks with pronounced intensities in the case of dicationic such as the new peak at 1655 cm^{-1}, and a failover in intensity from the monocationic and dicationic between the spectral regions 3200-2800 cm^{-1} and 3500-3200 cm^{-1}. The number of vibrational modes in the spectral region 3500-3200 cm^{-1} also increased, which can be explained by an increase in the number of N–H bonds. Therefore, these spectral regions are sensitive to the change of the number of imidazolium rings.

Such as the FT-RAMAN spectroscopy, we also have for FTIR/ATR spectroscopy an indicator of the existence of the order for the dicationic. This indicator is represented by the peaks in the spectrum of the dicationic being slightly narrower than the peaks in the spectrum of the monocationic.

Acknowledgment

The authors thank the ATRST-DGRSDT for the financial support. We would like to thank Quentin Arnould, technician of Walloon Agricultural Research Center (CRA-W), who participated to FT-RAMAN and FTIR/ATR measurements.

References

[1] J.M. Crosthwaite, M.J. Muldoon, J.K. Dixon, J.L. Anderson, J.F. Brennecke, Phase transition and decomposition temperatures, heat capacities and viscosities of pyridinium ionic liquids, J. Chem. Thermodyn. 37 (6) (2005) 559–568.
[2] J.D. Holbrey, K.R. Seddon, The phase behaviour of 1-alkyl-3-methylimidazolium tetrafluoroborates; ionic liquids and ionic liquid crystals, J. Chem. Soc. Dalton Trans. (13) (1999) 2133–2140.
[3] R. Hagiwara, Y. Ito, Room temperature ionic liquids of alkylimidazolium cations and fluoroanions, J. Fluor. Chem. 105 (2) (2000) 221–227.
[4] F. Endres, M. Bukowski, R. Hempelmann, H. Natter, Electrodeposition of nanocrystalline metals and alloys from ionic liquids, Angew. Chem. Int. Ed. 42 (29) (2003) 3428–3430.
[5] H. Ohno, Electrochemical Aspects of Ionic Liquids, John Wiley & Sons, 2011.
[6] M. Freemantle, An Introduction to Ionic Liquids, Royal Society of chemistry, 2010.
[7] A.J. Walker, N.C. Bruce, Cofactor-dependent enzyme catalysis in functionalized ionic solvents, Chem. Commun. (22) (2004) 2570–2571.
[8] K. Noack, P.S. Schulz, N. Paape, J. Kiefer, P. Wasserscheid, A. Leipertz, The role of the C2 position in interionic interactions of imidazolium based ionic liquids: a vibrational and NMR spectroscopic study, Phys. Chem. Chem. Phys. 12 (42) (2010) 14153–14161.
[9] A.M. Moschovi, S. Ntais, V. Dracopoulos, V. Nikolakis, Vibrational spectroscopic study of the protic ionic liquid 1-H-3-methylimidazolium bis (trifluoromethanesulfonyl) imide, Vib. Spectrosc. 63 (2012) 350–359.
[10] T. Moumene, E.H. Belarbi, B. Haddad, D. Villemin, O. Abbas, B. Khelifa, S. Bresson, Vibrational spectroscopic study of ionic liquids: comparison between monocationic and dicationic imidazolium ionic liquids, J. Mol. Struct. 1065 (2014) 86–92.
[11] K. Malek, A. Puc, G. Schroeder, V.I. Rybachenko, L.M. Proniewicz, FT-IR and FT-Raman spectroscopies and DFT modelling of benzimidazolium salts, Chem. Phys. 327 (2) (2006) 439–451.
[12] J. Kiefer, J. Fries, A. Leipertz, Experimental vibrational study of imidazolium-based ionic liquids: Raman and infrared spectra of 1-ethyl-3-methylimidazolium bis (trifluoromethylsulfonyl) imide and 1-ethyl-3-methylimidazolium ethylsulfate, Appl. Spectrosc. 61 (12) (2007) 1306–1311.
[13] T. Moumene, E.H. Belarbi, B. Haddad, D. Villemin, O. Abbas, B. Khelifa, S. Bresson, Study of imidazolium dicationic ionic liquids by Raman and FTIR spectroscopies: the effect of the nature of the anion, J. Mol. Struct. 1083 (2015) 179–186.
[14] T.C. Penna, L.F. Faria, J.R. Matos, M.C. Ribeiro, Pressure and temperature effects on intermolecular vibrational dynamics of ionic liquids, J. Chem. Phys. 138 (10) (2013) 104503.
[15] G. Socrates, Infrared and Raman Characteristic Group Frequencies: Tables and Charts, John Wiley & Sons, 2004.
[16] M. Koel, Ionic Liquids in Chemical Analysis, CRC Press, 2008.
[17] K. Malek, E. Podstawka, J. Milecki, G. Schroeder, L.M. Proniewicz, Structural features of the adenosine conjugate in means of vibrational spectroscopy and DFT, Biophys. Chem. 142 (1) (2009) 17–26.
[18] S. Bresson, D. Rousseau, S. Ghosh, M.E. Marssi, V. Faivre, Raman spectroscopy of the polymorphic forms and liquid state of cocoa butter, Eur. J. Lipid Sci. Technol. 113 (8) (2011) 992–1004.